Mössbauer spectrum (4 K) IS = 3.47 mm s^{-1} and QS 6.52 mm s^{-1}, IS = 4.24 mm s^{-1} and QS = 8.06 mm s^{-1}. Anal. Calcd for $C_{30}H_{33}Au_2BrP_2$ (929.4): Au, 42.39; P, 6.67. Found: Au, 40.61; P, 6.71.

μ,μ′-Bis[diphenylphosphonium bis(methylido)][dimethylgold(III)]gold(I) (4b). The primary ether extract in the preparation of **3b** (above) contained mainly **4b**, which could be recrystallized from toluene: 180 mg (13%) yield; mp 175–180 °C dec; ^{1}H NMR ($CDCl_3$) δ −0.35 (s, $AuCH_3$), 1.24 and 1.85 ($A_2A'_2XX'$, N = 13.0 and 13.4 Hz, respectively, CH_2P), 7.25–8.05 (m, C_6H_5); ^{31}P NMR δ 32.0 (s) {^{1}H}; ^{13}C NMR δ 8.0 (s, CH_3Au); 8.4 and 11.4 (AXX′, N = 47.9 and 48.8 Hz, respectively, CH_2P), 127.2–131.7 (m, C_6H_5). Anal. Calcd for $C_{30}H_{34}Au_2P_2$ (850.5): C, 42.37; H, 4.03. Found: C, 42.50; H, 4.19.

Structure Determination of 3b·$C_6H_5CH_3$. Suitable single crystals were obtained from toluene and sealed under argon at dry ice temperature into a glass capillary. Diffractometer measurements (Syntex P2$_1$) indicated a triclinic unit cell which was confirmed by axial photographs. Reduced cell calculations (TRACER) did not indicate any higher symmetry. Exact cell dimensions and their esd's were obtained by a least-squares fit of the parameters of the orientation matrix to the setting angles of 15 high order reflections from various parts of reciprocal space accurately centered on the diffractometer. Pertinent crystal data as well as a summary of intensity data collection and refinement are given in Table I. Data collection and refinement procedures followed closely those described in ref 31.

A total of 6055 unique intensity data were collected on an automated four-circle diffractometer (Syntex P2$_1$) at −40 °C. After correction for Lp effects and for those of absorption (empirical, based on ψ scans of seven reflections near $\chi = 90°$), 964 structure factors with $F_o \le 4.0\sigma(F_o)$ were deemed "unobserved" and not used in all further calculations. A total of 53 structure factors that were evidently mismeasured were additionally suppressed. The structure was solved by Patterson methods and completed by Fourier syntheses. Twelve out of a total of 36 hydrogen atom positions were taken from difference maps, and the rest was calculated at idealized geometrical positions as were those at the toluene molecule (XANADU). Refinement by full-matrix least-squares methods converged at $R = \sum(||F_o| - |F_c||)/\sum|F_o| = 0.044$ and $R_w = [\sum w(|F_o| - |F_c|)^2/\sum wF^2]^{1/2} = 0.053$. Thereby all non-hydrogen atoms were refined with anisotropic thermal parameters, with the exception of the toluene molecule which was refined as rigid group with individual isotropic thermal parameters. The H atoms were included in the structure factor calculations as fixed atom contributions and unit weights were used throughout (SHELX 76). A final difference synthesis showed maxima near the toluene and the Au atoms and was otherwise featureless. Reference 31 also contains the sources of the scattering factors and references to the programs used. Table II contains the atomic coordinates; Table III summarizes important distances and angles. Figure 2 gives a view of the molecular structure.

Acknowledgment. This work was generously supported by Deutsche Forschungsgemeinschaft, Bonn-Bad Godesberg, Fonds der Chemischen Industrie, Frankfurt/Main, and Degussa AG, Hanau-Wolfgang. We are grateful to Prof. F. E. Wagner for the Mössbauer measurements.

Registry No. **1b**, 81457-56-9; **2a**, 80387-84-4; **2b**, 80387-83-3; **2c**, 90742-64-6; **3a**, 102133-45-9; **3b**, 102133-46-0; **3b**·$C_6H_5CH_3$, 102133-49-3; **4a**, 55744-47-3; **4b**, 102133-48-2; **5**, 102133-47-1; $(CH_3)_3PAuCl$, 15278-97-4; $CH_3(C_6H_5)_2P{=}CH_2$, 4554-22-7; CH_2Br_2, 74-95-3.

Supplementary Material Available: Tables of anisotropic temperature factors, H atom coordinates, and observed and calculated structure factor amplitudes for **3b**·$C_6H_5CH_3$ (28 pages). Ordering information is given on any current masthead page.

---

(31) Schmidbaur, H.; Schier, A.; Frazão, C. M. F.; Müller, G. *J. Am. Chem. Soc.* 1986, *108*, 976.

X-ray Crystal Structure and Molecular Dynamics of (Indenyl)bis(ethylene)rhodium(I): 500-MHz NMR Spectra and EHMO Calculations

Michael Mlekuz,† Peter Bougeard,† Brian G. Sayer,† Michael J. McGlinchey,*† Charles A. Rodger,‡ Melvyn Rowen Churchill,*§ Joseph W. Ziller,§ Sung-Kwon Kang,⊥ and Thomas A. Albright*⊥

Department of Chemistry, McMaster University, Hamilton, Ontario L8S 4M1, Canada, Bruker Spectrospin, 555, Steeles Avenue East, Milton, Ontario L9T 1Y6, Canada, Department of Chemistry, University at Buffalo, State University of New York, Buffalo, New York, 14214, and Department of Chemistry, University of Houston, Houston, Texas 77004

Received August 2, 1985

(Indenyl)bis(ethylene)rhodium(I) crystallizes in the monoclinic space group $P2_1/n$ with a = 7.8387 (19) Å, b = 10.9886 (22) Å, c = 25.9379 (78) Å, β = 98.178 (22)°, V = 2211.5 (10) Å^3, and Z = 8. The $Rh(C_2H_4)_2$ moiety is displaced from the center of the five-membered ring toward an η^3-bonding mode. The 500-MHz DNMR spectra of the 1-methylindenyl analogue allow an evaluation of the ethylene rotation barrier and also of ML_2 rotation about the Rh–indenyl axis. Extended Hückel molecular orbital calculations were used to probe the mechanisms of these rotation processes.

Introduction

The use of NMR spectroscopy to measure rotational barriers in metal–olefin complexes was first discussed more than 20 years ago in a now classic paper by Cramer.[1] He noted that in the molecule $(C_5H_5)Rh(C_2H_4)_2$ (**1**) the alkene protons could be distinguished by their relative orientations with respect to the cyclopentadienyl ring. Thus the "outside" and "inside" protons could, in principle, be interconverted by a formal rotation about an axis joining the rhodium to the center of the carbon–carbon double bond.

---

† McMaster University.

‡ Bruker Spectrospin.

§ University of Buffalo.

⊥ University of Houston.

(1) Cramer, R. *J. Am. Chem. Soc.* 1964, *86*, 217.

Table I. Interatomic Distances (Å) for the Two Independent $(C_9H_7)Rh(C_2H_4)_2$ Molecules

molecule 1		molecule 2	
(A) Rhodium–Ethylene Distances			
Rh(1)–C(1A)	2.164 (8)	Rh(2)–C(2A)	2.148 (7)
Rh(1)–C(1B)	2.119 (9)	Rh(2)–C(2B)	2.142 (8)
Rh(1)–C(1C)	2.147 (8)	Rh(2)–C(2C)	2.147 (8)
Rh(1)–C(1D)	2.134 (8)	Rh(2)–C(2D)	2.155 (8)
R(1)···midpoint (1A,1B)	2.026	Rh(2)···midpoint (2A,2B)	2.030
Rh(1)···midpoint (1C,1D)	2.028	Rh(2)···midpoint (2C,2D)	2.040
(B) Rhodium–Carbon (η^5-C_5 system) Distances			
Rh(1)–C(11)	2.358 (7)	Rh(2)–C(21)	2.355 (7)
Rh(1)–C(16)	2.362 (7)	Rh(2)–C(26)	2.352 (7)
Rh(1)–C(17)	2.176 (8)	Rh(2)–C(27)	2.182 (8)
Rh(1)–C(18)	2.215 (8)	Rh(2)–C(28)	2.224 (8)
Rh(1)–C(19)	2.206 (7)	Rh(2)–C(29)	2.214 (7)
Rh(1)···centroid (Cp 1)	1.889	Rh(2)···centroid (Cp 2)	1.915
(C) Distances within η^2-C_2H_4 Ligands			
C(1A)–C(1B)	1.387 (13)	C(2A)–C(2B)	1.387 (12)
C(1C)–C(1D)	1.368 (13)	C(2C)–C(2D)	1.366 (14)
(D) Distances with the η^5-C_5 Systems			
C(16)–C(11)	1.448 (10)	C(26)–C(21)	1.432 (10)
C(16)–C(17)	1.428 (11)	C(26)–C(27)	1.437 (11)
C(17)–C(18)	1.419 (12)	C(27)–C(28)	1.417 (12)
C(18)–C(19)	1.408 (11)	C(28)–C(29)	1.407 (12)
C(19)–C(11)	1.441 (10)	C(29)–C(21)	1.444 (11)
(E) Distances within the C_6 Rings			
C(11)–C(12)	1.399 (12)	C(21)–C(22)	1.401 (12)
C(12)–C(13)	1.335 (15)	C(22)–C(23)	1.368 (14)
C(13)–C(14)	1.390 (19)	C(23)–C(24)	1.389 (17)
C(14)–C(15)	1.379 (15)	C(24)–C(25)	1.373 (15)
C(15)–C(16)	1.406 (12)	C(25)–C(26)	1.427 (12)

Variable-temperature NMR studies[2] elucidated this barrier to alkene rotation, ΔG^*, as 15 kcal mol^{-1}. Furthermore, it was shown that replacement of one of the ethylenes by ligands which could compete successfully with the remaining C_2H_4 moiety for π-back-donated electron density weakened the Rh–C_2H_4 bond and lowered the barrier to rotation.[3,4] In agreement with this picture, the incorporation of electron-withdrawing groups in the cyclopentadienyl ring lowered the barrier whereas, in the pentamethylcyclopentadienyl analogue, the ΔG^* value increased to >17 kcal mol^{-1}.[5] Since that time, this NMR approach has been applied to many metal–alkene complexes,[6] and theoretical calculations have accounted for the variation of rotational barriers with molecular geometry and metal electron count.[7]

In recent years, a vast number of cyclopentadienyl derivatives of rhodium have been prepared, but the most interesting may well be the indenyl derivatives, (C_9H_7)-RhL_2, which show enormously enhanced reactivity.[8,9] This phenomenon has been rationalized in terms of a slippage from an η^5- to an η^3-bonding mode; indeed, this interpretation has received convincing support from the recent kinetic studies of Basolo, Ji, and Rerek,[10] as well as from the X-ray data of Faller, Crabtree, and Habib.[11] Furthermore, the barrier to ethylene rotation in $(C_9H_7)Rh$-$(C_2H_4)_2$ (2) has been reported to be much lower (10.5 kcal mol^{-1}) than in the cyclopentadienyl complex 1.[8,12] In contrast, replacement of the cyclopentadienyl group by indenyl in $[CpFe(CO)_2(C_2H_4)]^+$, $CpFe(CO)(C_2H_4)SnR_3$, and $CpW(CO)_2(C_2H_4)CH_3$ has an almost negligible effect.[13-15] For these reasons, we decided to carry out X-ray

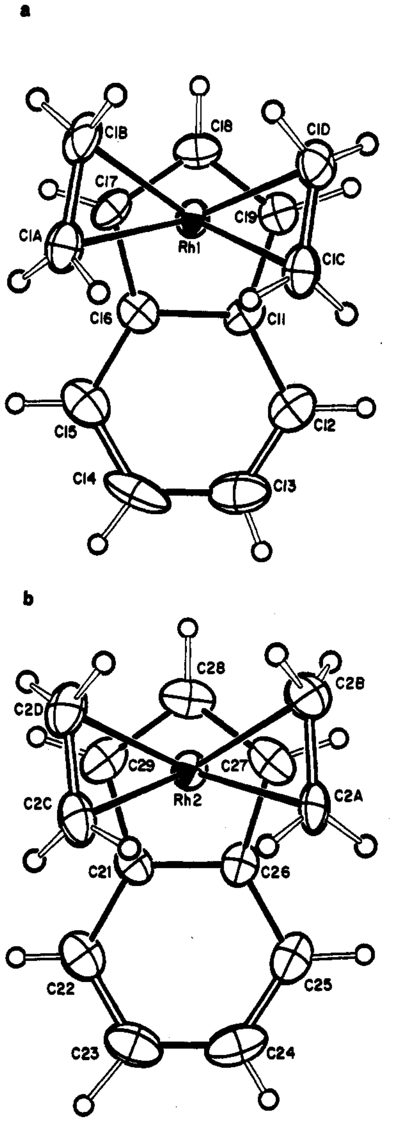

Figure 1. ORTEP-II diagrams of the $(\eta^5$-$C_9H_7)Rh(\eta^2$-$C_2H_4)_2$ molecules with hydrogen atoms artificially reduced: (a) molecule 1; (b) molecule 2.

---

[2] Cramer, R.; Kline, J. B.; Roberts, J. D. *J. Am. Chem. Soc.* **1969**, *91*, 2519.

[3] Guggenberger, L. J.; Cramer, R. *J. Am. Chem. Soc.* **1972**, *94*, 3779.

[4] Cramer, R.; Mrowca, J. J. *Inorg. Chim. Acta* **1971**, *5*, 528.

[5] Cramer, R.; Reddy, G. S. *Inorg. Chem.* **1973**, *12*, 346.

[6] Mann, B. E. In *Comprehensive Organometallic Chemistry*; Wilkinson, G., Stone, F. G. A., Abel, E. W., Eds.; Pergamon Press: Oxford, 1982; Vol. 3, pp 103–109.

[7] (a) Albright, T. A.; Hoffmann, R.; Thibeault, J. C.; Thorn, D. L. *J. Am. Chem. Soc.* **1979**, *101*, 3801. (b) Albright, T. A. *Acc. Chem. Res.* **1982**, *15*, 149.

[8] (a) Caddy, P.; Green, M.; O'Brien, E.; Smart, L. E.; Woodward, P. *Angew. Chem., Int. Ed. Engl.* **1977**, *16*, 648. (b) Caddy, P.; Green, M.; O'Brien, E.; Smart, L. E.; Woodward, P. *J. Chem. Soc., Dalton Trans.* **1980**, 962.

[9] Werner, H.; Feser, R. *Z. Naturforsch., B: Anorg. Chem., Org. Chem.* **1980**, *35B*, 689.

[10] (a) Rerek, M. E.; Ji, L.-N.; Basolo, F. *J. Chem. Soc., Chem. Commun.* **1983**, 1208. (b) Ji, L.-N.; Rerek, M. E.; Basolo, F. *Organometallics* **1984**, *3*, 740.

[11] (a) Faller, J. W.; Crabtree, R. H.; Habib, A. *Organometallics* **1985**, *4*, 929 and references therein. (b) Merola, J. S.; Kacmarcik, R. T.; Van Engan, D. *J. Am. Chem. Soc.* **1986**, *108*, 329.

[12] Eshtiagh-Hosseini, H.; Nixon, J. F. *J. Less-Common Met.* **1978**, *61*, 107.

[13] Faller, J. W.; Johnson, B. V. *J. Organomet. Chem.* **1975**, *88* 101.

[14] Faller, J. W.; Johnson, B. V.; Schaeffer, C. D., Jr. *J. Am. Chem. Soc.* **1976**, *98*, 1395.

[15] Alt, H. G.; Schwarzle, J. A.; Kreiter, C. G. *J. Organomet. Chem.* **1978**, *153*, C7.

Table II. Interatomic Angles (deg) for $(C_9H_7)Rh(C_2H_4)_2$

molecule 1		molecule 2	
(A) Angles about the Rhodium Atoms			
C(1A)-Rh(1)-C(1B)	37.8 (4)	C(2A)-Rh(2)-C(2B)	37.7 (3)
C(1A)-Rh(1)-C(1C)	89.2 (3)	C(2A)-Rh(2)-C(2C)	88.3 (3)
C(1A)-Rh(1)-C(1D)	103.0 (3)	C(2A)-Rh(2)-C(2D)	102.4 (3)
C(1B)-Rh(1)-C(1C)	99.7 (4)	C(2B)-Rh(2)-C(2C)	100.3 (3)
C(1B)-Rh(1)-C(1D)	89.6 (4)	C(2B)-Rh(2)-C(2D)	90.8 (3)
C(1C)-Rh(1)-C(1D)	37.3 (3)	C(2C)-Rh(2)-C(2D)	37.0 (3)
C(11)-Rh(1)-C(16)	35.7 (2)	C(21)-Rh(2)-C(26)	35.4 (3)
C(16)-Rh(1)-C(17)	36.4 (3)	C(26)-Rh(2)-C(27)	36.7 (3)
C(17)-Rh(1)-C(18)	37.7 (3)	C(27)-Rh(2)-C(28)	37.5 (3)
C(18)-Rh(1)-C(19)	37.1 (3)	C(28)-Rh(2)-C(29)	37.0 (3)
C(19)-Rh(1)-C(11)	36.6 (3)	C(26)-Rh(2)-C(21)	36.7 (3)
midpoint(1A,1B)-Rh(1)-midpoint(1C,1D)	96.0 (...)	midpoint(2A,2B)-Rh(2)-midpoint(2C,2D)	96.0 (...)
midpoint(1A,1B)-Rh(1)-centroid (Cp 1)	131.3 (...)	midpoint(2A,2B)-Rh(2)-centroid (Cp 2)	131.7 (...)
midpoint(1C,1D)-Rh(1)-centroid (Cp 1)	132.7 (...)	midpoint(2C,2D)-Rh(2)-centroid (Cp 2)	132.3 (...)
(B) Angles within Indenyl Groups			
C(11)-C(12)-C(13)	119.4 (9)	C(21)-C(22)-C(23)	119.2 (9)
C(12)-C(13)-C(14)	122.4 (12)	C(22)-C(23)-C(24)	120.8 (10)
C(13)-C(14)-C(15)	121.1 (11)	C(23)-C(24)-C(25)	123.0 (10)
C(14)-C(15)-C(16)	118.6 (9)	C(24)-C(25)-C(26)	117.4 (9)
C(15)-C(16)-C(11)	118.9 (7)	C(25)-C(26)-C(21)	119.4 (7)
C(15)-C(16)-C(17)	134.3 (7)	C(25)-C(26)-C(27)	132.9 (7)
C(16)-C(17)-C(18)	109.1 (7)	C(26)-C(27)-C(28)	108.5 (7)
C(17)-C(18)-C(19)	107.5 (7)	C(27)-C(28)-C(29)	107.4 (7)
C(18)-C(19)-C(11)	108.7 (7)	C(28)-C(29)-C(21)	109.3 (7)
C(11)-C(16)-C(17)	106.7 (6)	C(21)-C(26)-C(27)	107.6 (6)
C(16)-C(11)-C(19)	107.0 (6)	C(26)-C(21)-C(29)	106.4 (6)
C(12)-C(11)-C(16)	119.6 (7)	C(22)-C(21)-C(26)	120.2 (7)
C(12)-C(11)-C(19)	133.4 (7)	C(22)-C(21)-C(29)	133.3 (7)
(C) Angles Involving Ethylene Ligands			
Rh(1)-C(1A)-C(1B)	69.4 (5)	Rh(2)-C(2A)-C(2B)	70.9 (5)
Rh(1)-C(1B)-C(1A)	72.9 (6)	Rh(2)-C(2B)-C(2A)	71.4 (5)
Rh(1)-C(1C)-C(1D)	70.9 (5)	Rh(2)-C(2C)-C(2D)	71.8 (5)
Rh(1)-C(1D)-C(1C)	71.9 (5)	Rh(2)-C(2D)-C(2C)	71.2 (5)

crystallographic and high field NMR studies on 2 and the 1-methylindenyl analogue 3.

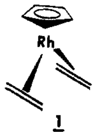

1

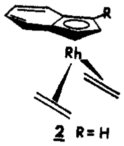

2 R = H
3 R = Me

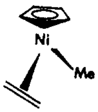

4

Results and Discussion

Crystal Structure of $(C_9H_7)Rh(C_2H_4)_2$. The crystal consists of discrete molecular units of $(C_9H_7)Rh(C_2H_4)_2$ which are mutually separated by normal van der Waals' distances; there are no abnormally short intermolecular contacts. The crystallographic asymmetric unit consists of two independent molecules (cf., parts a and b of Figure 1). Interatomic distances and angles are collected in Tables I and II. Stereoscopic views of the two molecules are provided in parts a and b of Figure 2.

The two molecules are chemically equivalent and correspond to $(\eta^5-C_9H_7)Rh(\eta^2-C_2H_4)_2$ systems, each having formally a count of 18 outer valence electrons. The ethylene ligands have carbon–carbon bond lengths of 1.387 (13) Å for C(1A)–C(1B), 1.368 (13) Å for C(1C)–C(1D), 1.387 (12) Å for C(2A)–C(2B), and 1.366 (14) Å for C(2C)–C(2D); the average value[16] of 1.377 [12] Å shows these bonds to be lengthened significantly relative to the typical uncoordinated C═C distances of 1.335 ± 0.005 Å.[17] The hydrogen atoms of the η^2-C_2H_4 ligands are not coplanar with their C═C systems but are displaced so as to be further away from the central rhodium atoms; since esd's on C–H distances are ~0.07 Å, it is not possible to discuss this feature in quantitative terms. However, all observed geometric features of the η^2-C_2H_4 are compatible with the accepted mode of interaction of an olefin with a transition metal which contains a component of $d\pi$–π^* metal→olefin back-donation.[18]

Rh–C(olefin) distances range from 2.119 (9) through 2.164 (8) Å, averaging 2.145 [14] Å; the Rh···midpoint(olefin) distances show closer agreement with values of 2.026, 2.028, 2.030, and 2.040 Å (average = 2.031 [6] Å). The two η^2-C_2H_4 ligands on each rhodium atom are disposed such that midpoint(1A,1B)–Rh–midpoint(1C,1D) = 96.0° and midpoint(2A,2B)–Rh–midpoint(2C,2D) = 96.0°.

Although the C_9H_7 ligand is bonded to rhodium in the η^5 mode, there is clearly some deviation from the possible regular C_{5v} symmetry for the η^5-C_5Rh moiety. Each rhodium atom is associated with three "short" Rh–C(cyclopentadienyl) distances and two "long" Rh–C(cyclopentadienyl) distances. The "short" Rh–C distances range from 2.176 (8) through 2.224 (8) Å (average = 2.203 [19] Å), while the "long" Rh–C distances range from 2.352 (7) through 2.362 (7) Å (average = 2.357 [4] Å); in each case, the "long" Rh–C bonds involve the bridgehead carbon atoms (i.e., C(11) and C(16); C(21) and C(26)). The

---

[16] Estimated standard deviations of average values are calculated by the scatter formula below and are given in square brackets.

$$[\sigma] = [\sum(d_i - \bar{d})^2/(N - 1)]^{1/2}$$

Here d_i is the *i*th of *N* equivalent distances, and $\bar{d}$ is the average value.

[17] *Spec. Publ.—Chem. Soc.* **1965**, *No. 18*, S16s.

[18] Chatt, J.; Duncanson, L. A. *J. Chem. Soc.* **1953**, 2939.

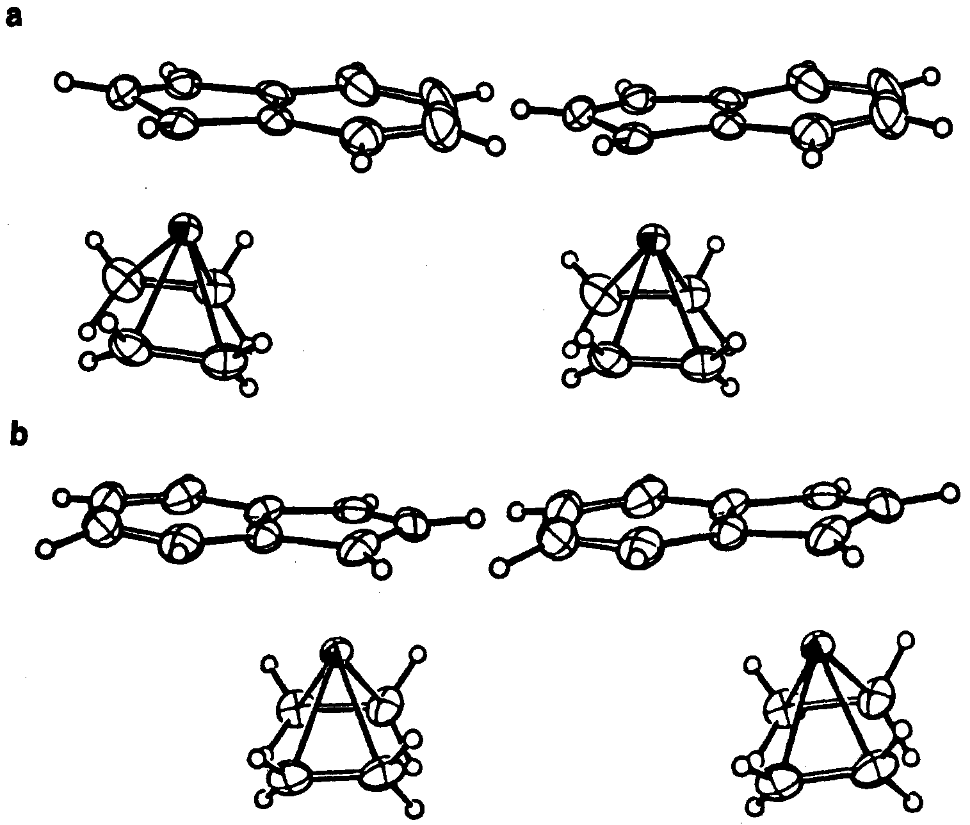

Figure 2. Stereoviews of the (η^5-C_9H_7)Rh(η^2-C_2H_4)$_2$ molecules: (a) molecule 1; (b) molecule 2.

molecule thus shows some distortion from a regular η^5-cyclopentadienyl complex (structure 5) toward an η^3-allyl system (structure 6). In each molecule, C–C bond lengths

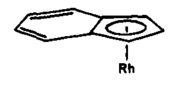

5

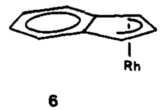

6

in the η^3-allyl system are shorter than those around the remainder of the five-membered ring (i.e., 1.407 (12)–1.419 (12) Å, averaging 1.413 [6] Å, vis-à-vis 1.428 (11)–1.448 (10) Å, averaging 1.438 [8] Å, respectively). The η^5-C_5 rings are bent across C(17)···C(19) and C(27)···C(29) with dihedral angles of 9.27° and 8.59° (see Table III).

We thus appear to have evidence for some localization in the η^5-cyclopentadienyl system. This was first suggested by Dahl and Wei in 1963[19] and was shortly thereafter discussed by Bennett, Churchill, Gerloch, and Mason (in 1964)[20] and Churchill (in 1965).[21] The accuracy of these early (photographic) measurements was limited, but the idea of localization of charge in an η^5-C_5 system in a low-symmetry local environment dates back to that time. Since then, the structures of several indenyl–metal complexes have been determined, and they show localized bonding to different extents. The first unequivocal example of an η^3-indenyl complex is that very recently reported by Merola.[11b] Electronic reasons for such distortions are outlined below.

Other distances and angles are within the expected ranges—see Tables II and III.

Scheme I. The Interconversion of Ethylene Proton Environments in (C_9H_7)Rh(C_2H_4)$_2$: (i) Ethylene Rotation; (ii) Indenyl Rotation

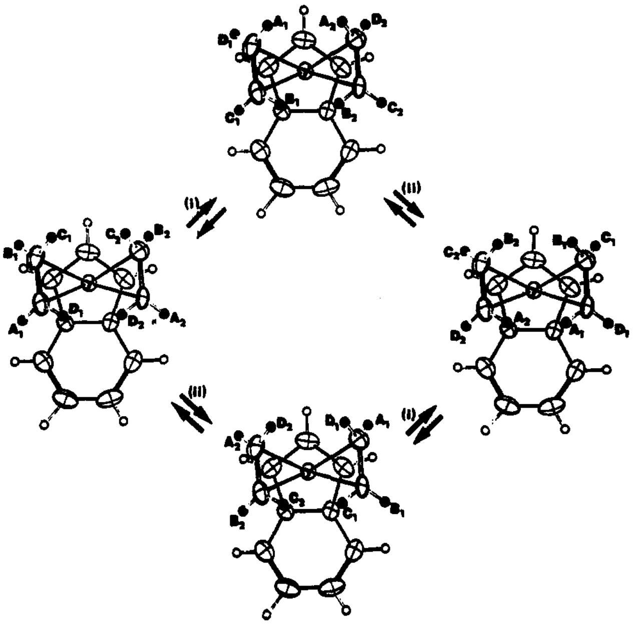

NMR Spectroscopic Studies. It had been previously reported that the 60-MHz ¹H NMR spectrum of (C_9H_7)Rh(C_2H_4)$_2$ (2) showed a single resonance (doublet split by ^{103}Rh) for the ethylene protons at +50 °C and that this split to give two multiplets at −90 °C.[12] By analogy with the earlier work of Cramer[1-5] this was rationalized in terms of a slowing of the ethylene rotation on the NMR time scale. The barrier was estimated to be 10.3 kcal mol^{-1}. One must, however, exercise some caution since the crystal structure of 2 shows that there are not two but four proton environments. Complete equilibration of these protons requires not only rotation about the alkene–rhodium axis but also rotation of the Rh(C_2H_4)$_2$ fragment about the metal–indenyl axis. As shown in Scheme I, the two rota-

---

[19] Dahl, L. F.; Wei, C. H. *Inorg. Chem.* **1963**, *2*, 713.

[20] Bennett, M. J.; Churchill, M. R.; Gerloch, M.; Mason, R. *Nature (London)* **1964**, *201*, 1318.

[21] Churchill, M. R. *Inorg. Chem.* **1965**, *4*, 1734.

Table III. Selected Intramolecular Planes, Atomic Deviations Therefrom, and Dihedral Angles for $(C_9H_7)Rh(C_2H_4)_2$

atom	dev, Å	atom	dev, Å
(A) The C(17)–C(18)–C(19) Plane			
$(0.7160X - 0.6686Y - 0.2007Z + 5.4739 = 0)$			
C(17)*	0.000	C(11)	–0.211 (7)
C(18)*	0.000	C(16)	–0.233 (7)
C(19)*	0.000	Rh(1)	1.822 (1)
(B) The C(17)–C(16)–C(11)–C(19) Plane			
$(0.7301X - 0.6822Y - 0.0403Z + 3.0460 = 0)$			
C(17*)	0.007 (8)	C(18)	–0.134 (8)
C(16)*	–0.008 (7)	Rh(1)	1.867 (1)
C(11*)	0.008 (7)		
C(19)*	–0.006 (7)		
(C) The Six-Membered Ring (Molecule 1)			
$(0.7339X - 0.6773Y - 0.0505Z + 3.2024 = 0)$			
C(11)*	0.002 (7)	C(14)*	–0.002 (13)
C(12)*	0.006 (9)	C(15)*	0.009 (9)
C(13)*	–0.014 (14)	C(16)*	–0.006 (7)
(D) The C(27)–C(28)–C(29) Plane			
$(0.7209X - 0.6596Y - 0.2126Z + 3.5357 = 0)$			
C(27)*	0.000	C(21)	0.192 (7)
C(29)*	0.000	C(26)	0.220 (7)
C(29)*	0.000	Rh(2)	–1.831 (1)
(E) The C(27)–C(26)–C(21)–C(29) Plane			
$(0.7368X - 0.6730Y - 0.0642Z + 0.0204 = 0)$			
C(27)*	–0.008 (8)	C(28)	0.125 (8)
C(26)*	0.010 (7)	Rh(2)	–1.875 (1)
C(21)*	–0.010 (7)		
C(29)*	0.008 (8)		
(F) The Six-Membered Ring (Molecule 2)			
$(0.7401X - 0.6686Y - 0.0719Z + 0.1805 = 0)$			
C(21)*	–0.004 (7)	C(24)*	0.014 (12)
C(22)*	0.000 (10)	C(25)*	–0.015 (9)
C(23)*	–0.002 (11)	C(26)*	0.008 (7)
(G) Dihedral Angles			
molecule 1		molecule 2	
A/B	9.27°	D/E	8.59°
B/C	0.69°	E/F	0.55°
A/C	8.69°	D/F	8.16°

tion mechanisms interconnect different proton environments. Specifically, rotation about the metal–indenyl vector interconverts A_1 and B_2, B_1 and A_2, C_1 and D_2, and D_1 and C_2. In contrast, alkene rotation interconverts A_1 and C_1, B_1 and D_1, A_2 and C_2, and B_2 and D_2. It is important to realize that the A_1 proton can gain access only to the B_2, C_1, and D_2 positions, and it is merely the presence of a molecular mirror plane which renders the A_1 proton equivalent to A_2 (and hence to B_1, C_2, and D_1). In the absence of a molecular mirror plane the eight protons will fall into two noninterconvertible sets of four. Of course, the phenomenon of diastereotopicity in chiral molecules is well-understood,[22] and we merely wish to emphasize that in this case each of the two sets of four discussed above is made up of a trans-related pair of protons from different ethylenes; we do not simply have diastereotopic ethylenes each providing a set of four interconvertible protons.

$(C_5H_5)Rh(C_2H_4)_2$ (1) has effective C_{2v} symmetry, and alkene rotation alone suffices to equilibrate the "outside" (δ 2.86) and "inside" (δ 1.03) proton environments. These

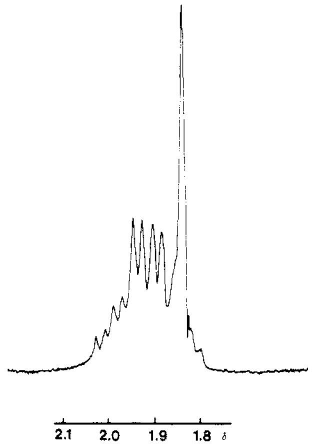

Figure 3. 90-MHz ^1H NMR spectrum of the ethylene protons of **3** at room temperature.

assignments in which the "inside" protons are more shielded than the "outside" ones was based not only on a detailed analysis of the coupling constants[2] but also on comparisons with coordinated 1,5-hexadiene.[1] These assignments have been elegantly confirmed by Benn, who showed that in the closely related molecule $(C_5H_5)Ni(C_2H_4)CH_3$ (**4**), the lower field protons of ethylene experience an appreciable nuclear Overhauser effect from the hydrogens in the cyclopentadienyl ring while the higher field ethylene protons are clearly proximate to the methyl group.[23] A perhaps rather naive explanation would relate these shifts to the anisotropic shielding effect of the C_5H_5 ring which, analogously to benzene,[24] should shield protons above the ring plane and deshield those close to the plane of the ring. The net result for a range of such molecules is that the inner protons generally resonate 1–1.5 ppm to higher field (lower frequency) than their outer partners. Interestingly, Faller has used ring current calculations to determine the orientation of olefins proximate to a complexed indenyl ligand.[13]

Clearly for $(C_9H_7)Rh(C_2H_4)_2$ at 60 MHz only one process (presumed to be alkene rotation) can be detected,[12] and, even at 250 MHz, no further decoalescence occurs. To investigate this process, we prepared bis(ethylene)(η^5-1-methylindenyl)rhodium(I) (**3**)—a chiral molecule satisfying the criteria outlined above for splitting the eight ethylenic protons into two noninterconvertible sets of four. The 90-MHz ^1H spectrum of **3** at room temperature exhibits two peaks for the ethylene resonances (Figure 3) each doublet split by ^{103}Rh ($I = ^1/_2$; 100% abundant). At 250 MHz, one sees two clearly separated resonances which only show rhodium–hydrogen coupling above 50 °C. The observation of two proton environments at high temperature verifies the intramolecular nature of the process. If olefin dissociation were to occur, all four hydrogens in the liberated C_2H_4 would become equivalent and the diastereotopic character of the protons would be lost. In an attempt to obtain the limiting low-temperature spectrum, the 500-MHz ^1H spectrum was recorded. At −108 °C, as shown in Figure 4a, the region assigned to the outside protons exhibits a 1:2:1 pattern while the corresponding inner hydrogens appear as a 1:1:1:1 broadened multiplet. It is noticeable that although the shift dispersion is of course not quite as good at 250 or 400 MHz, coupling between the ethylene protons is better resolved at comparable stages

---

[22] Mislow, K. *Introduction to Stereochemistry*; W. A. Benjamin: Reading, *Ma*, 1965.

[23] Benn, R. *Org. Magn. Reson.* **1983**, *21*, 723.

[24] (a) Johnson, C. E., Jr.; Bovey, F. A. *J. Chem. Phys.* **1958**, *29*, 1012. (b) Haigh, C. W.; Mallion, R. B. *Prog. Nucl. Magn. Reson. Spectrosc.* **1979**, *13*, 303. (c) Agarwal, A.; Barnes, J. A.; Fletcher, J. L.; McGlinchey, M. J.; Sayer, B. G. *Can. J. Chem.* 1977, *55*, 2575.

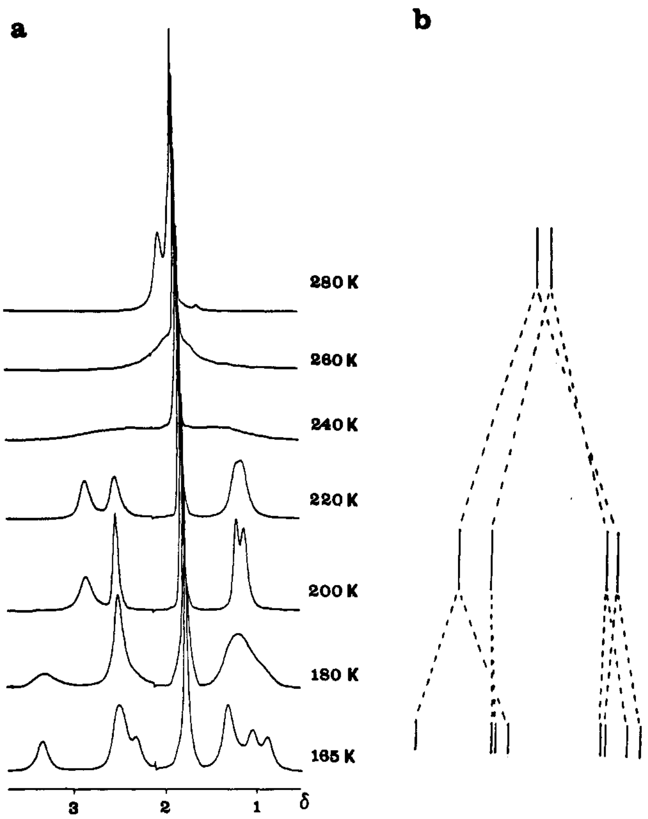

Figure 4. (a) Sections of the variable-temperature 500-MHz ^1H NMR spectra of $(CH_3\text{-}C_9H_6)Rh(C_2H_4)_2$ (**3**) in CD_2Cl_2. (b) Coalescence pattern of the ethylene protons of **3** over the temperature range 165–280 K.

of peak coalescence. This is not simply a question of resolution since the protons in the aromatic region are very clearly resolved at all fields. Rather we suspect that the broadening observed at 500 MHz is attributable to chemical shielding anisotropy. CSA effects are widespread at high fields when one is either observing directly or coupling to a spin $^1/_2$ nucleus with a large chemical shift range.[25] Such behavior is well-documented for ^{119}Sn, ^{123}Te, ^{129}Xe, and ^{195}Pt.

The coalescence pattern observed upon increasing the temperature is summarized in Figure 4b and follows that predicted at the outset. A crucial point is that the initial coalescence from eight proton environments (which occurs over the temperature range −108 to −70 °C and has a barrier $\Delta G^\ddagger$ (190 K) of 8.5 ± 0.4 kcal mol^{-1}) only involves interchange within the set of outer protons and within the set of inner protons. This confirms that it is indeed rotation about the metal–ring axis which is the lower activation energy process. In contrast, the higher energy exchange process ($\Delta G^\ddagger$ (240 K) = 10.4 ± 0.5 kcal mol^{-1}) involves only the interconversion of outer and inner proton environments; this must be the case for an olefin rotation process.

The ^{13}C NMR spectra measured at 125.72 MHz were entirely in accordance with the scenario described above. At room temperature the ethylenes (Figure 5) exhibit only a single resonance since the combination of two rotation processes allows each carbon access to all three other sites. At −53 °C alkene rotation has been stopped on the ^{13}C time scale, and two sharp peaks are observed. Again, the activation energy barrier was found to be 10.5 ± 0.5 kcal mol^{-1}. At −108 °C, one of the resonances has completely decoalesced ($\Delta G^\ddagger$ = 8.4 ± 0.5 kcal mol^{-1}), and the other has noticeably broadened. We reiterate that at −53 °C one is not seeing a peak due to each ethylene but rather each peak comprises a pair of carbons *from different ethylenes* but related by the twofold rotation about the rhodium-indenyl axis.

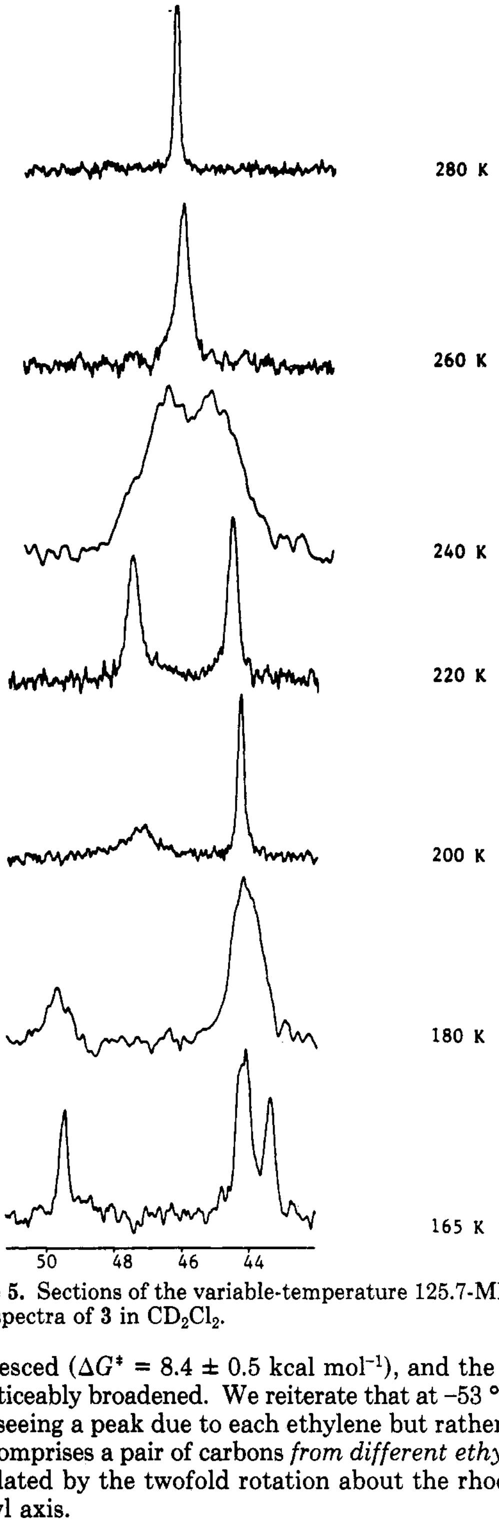

Figure 5. Sections of the variable-temperature 125.7-MHz ^{13}C NMR spectra of **3** in CD_2Cl_2.

We are aware of only one other published barrier to indenyl rotation about a ring-metal axis and that is in a bimetallic Rh–Cr complex;[26] in that case, the barrier was 11 kcal mol^{-1}. Rotation about a metal–cyclopentadienyl ring axis is normally extremely facile, but for rings bearing bulky substituents barriers in the range 8–13 kcal mol^{-1} has been reported.[27] It is of interest to note here that replacement of the two ethylene ligands in **3** by chelating diphosphines yield molecules containing diastereotopic phosphorus nuclei. Thus ^{31}P variable-temperature NMR

---

[25] Davies, J. A. In *The Chemistry of the Metal-Carbon Bond*; Hartley, F. R., Patai, S., Eds.; Wiley: Chichester, 1982; Vol. 1, p 827 and references therein.

[26] Barr, R. D.; Green, M.; Marder, T. B.; Stone, F. G. A. *J. Chem. Soc., Dalton Trans.* **1984**, 1261.

[27] Erker, G.; Mühlenbernd, T.; Benn, R.; Rufinska, A.; Tsay, Y.-H.; Krüger, C. *Angew. Chem., Int. Ed. Engl.* **1985**, *24*, 321 and references therein.

Table IV. Experimental Data for X-ray Diffraction Study of $(C_9H_7)Rh(C_2H_4)_2$

(A) Crystal Parameters at 21 °C (294 K)

cryst system: monoclinic
space group: $P2_1/n$
$a = 7.8387\ (19)$ Å
$b = 10.9886\ (22)$ Å
$c = 25.9379\ (78)$ Å
$\beta = 98.178\ (22)°$
$V = 2211.5\ (10)$ Å^3
$Z = 8$
mol wt = 274.2
ρ(calcd) = 1.65 g cm^{-3}

(B) Data Collection

diffractometer: Syntex $P2_1$
radiatn: Mo Kα ($\bar{\lambda} = 0.710730$ Å)
monochromator: pyrolytic graphite, equatorial, $2\theta(m) = 12.2°$, assumed 50% perfect
scan type: coupled θ(crystal)–2θ(counter)
scan width: symmetrical, $[1.8 + \Delta(\alpha_2 - \alpha_1)]°$
scan speed: 4.0° min^{-1}
reflectns collected: $+h,+k,\pm l$ for $2\theta = 4.0$–$45.0°$, 2915 unique data
absorptn coeff: $\mu = 14.6$ cm^{-1}; corrected by interpolation between experimental ψ scans of three close-to-axial reflections ($40\bar{2}$, $\bar{5}13$, $\bar{3}11$)

measurements allow evaluation of the barrier to ML_2 rotation about the indenyl–Rh axis. This phenomenon has also been observed by T. Marder et al.,[28] and full details will appear in a paper describing our joint efforts in this area.

It is interesting to speculate as to why the alkene rotation barrier is so much lower in the indenyl compounds **2** and **3** than in the cyclopentadienyl complex **1**. The problem of metal–ethylene rotational barriers has been the subject of theoretical calculations,[7] and the major contributory factors have been elucidated. It has been shown that to develop a sizeable barrier to rotation, one should have markedly different overlaps and energy separations between the metal fragment frontier orbitals and the ethylene π^* orbital in two orientations at right angles. Thus, in d^6 $ML_5(C_2H_4)$ octahedral systems, the barrier is small while in d^{10} $ML_2(C_2H_4)$ trigonal-planar molecules the barrier to rotation can be high. The most interesting case is that of the trigonal-bipyramidal complex $Fe(CO)_4(C_2H_4)$ where the barrier to ethylene rotation would be ca. 30 kcal mol^{-1} if the ML_4 fragment retained its geometry. In contrast, if the olefin rotation process is concomitant with a Berry pseudorotation of the molecule, the activation energy requirements are drastically reduced.[7]

Table V. Final Positional Parameters for $(C_9H_7)Rh(C_2H_4)_2$

atom	*x*	*y*	*z*	*B*(iso), Å^2
Rh(1)	0.40831 (7)	0.16912 (5)	0.60298 (2)	
Rh(2)	0.60117 (6)	0.18678 (5)	0.91279 (2)	
C(1A)	0.68554 (93)	0.18839 (79)	0.61905 (35)	
C(1B)	0.6301 (11)	0.1917 (10)	0.56583 (39)	
C(1C)	0.4352 (11)	−0.01987 (69)	0.62349 (37)	
C(1D)	0.3761 (12)	−0.01012 (69)	0.57143 (35)	
C(11)	0.19587 (83)	0.22988 (64)	0.65357 (27)	
C(12)	0.1608 (11)	0.17719 (88)	0.70003 (36)	
C(13)	0.2423 (16)	0.2184 (13)	0.74538 (46)	
C(14)	0.3652 (16)	0.3102 (13)	0.74834 (39)	
C(15)	0.4071 (11)	0.36505 (84)	0.70400 (38)	
C(16)	0.32149 (86)	0.32696 (63)	0.65536 (28)	
C(17)	0.3325 (11)	0.35960 (71)	0.60264 (31)	
C(18)	0.2031 (10)	0.29630 (75)	0.56919 (33)	
C(19)	0.13103 (87)	0.20905 (69)	0.59949 (29)	
C(2A)	0.32586 (88)	0.16983 (76)	0.89574 (33)	
C(2B)	0.3755 (10)	0.15701 (84)	0.94896 (33)	
C(2C)	0.5729 (11)	0.37703 (71)	0.89468 (39)	
C(2D)	0.6321 (11)	0.36599 (71)	0.94658 (39)	
C(21)	0.81264 (89)	0.13016 (66)	0.86130 (29)	
C(22)	0.8470 (12)	0.18539 (91)	0.81521 (38)	
C(23)	0.7604 (14)	0.1464 (10)	0.76861 (40)	
C(24)	0.6419 (14)	0.0519 (11)	0.76659 (41)	
C(25)	0.5999 (11)	−0.00451 (89)	0.81031 (38)	
C(26)	0.69020 (87)	0.03300 (66)	0.85941 (30)	
C(27)	0.6802 (11)	−0.00350 (68)	0.91211 (33)	
C(28)	0.8092 (10)	0.05949 (83)	0.94563 (30)	
C(29)	0.87951 (89)	0.14798 (80)	0.91559 (32)	
H(1A1)	0.7211 (86)	0.1089 (65)	0.6387 (26)	4.4 (17)
H(2A1)	0.6908	0.2624	0.6381	6.0
H(1B1)	0.6354 (89)	0.2596 (66)	0.5485 (27)	4.0 (19)
H(2B1)	0.647 (11)	0.1224 (79)	0.5442 (32)	6.6 (25)
H(1C1)	0.3459 (90)	−0.0310 (63)	0.6438 (27)	4.8 (19)
H(2C1)	0.5536	−0.0158	0.6376	6.0
H(1D1)	0.2603 (88)	−0.0175 (66)	0.5600 (27)	4.3 (19)
H(2D1)	0.4543	0.0042	0.5473	6.0
H(12)	0.0824 (93)	0.1062 (69)	0.6970 (27)	4.8 (19)
H(13)	0.244 (14)	0.1835 (94)	0.7739 (41)	9.5 (37)
H(14)	0.4204 (83)	0.3439 (59)	0.7766 (27)	3.5 (17)
H(15)	0.4920	0.4272	0.7062	6.0
H(17)	0.4053 (76)	0.4166 (59)	0.5942 (23)	2.9 (16)
H(18)	0.1758 (90)	0.3075 (65)	0.5359 (27)	4.4 (19)
H(19)	0.021 (13)	0.1577 (92)	0.5837 (39)	10.7 (33)
H(1A2)	0.3021 (69)	0.0981 (53)	0.8752 (21)	1.9 (13)
H(2A2)	0.3157	0.2481	0.8800	6.0
H(1B2)	0.349 (10)	0.2305 (74)	0.9702 (31)	6.7 (22)
H(2B2)	0.4293	0.0856	0.9642	6.0
H(1C2)	0.6493 (73)	0.3909 (53)	0.8743 (22)	1.9 (14)
H(2C2)	0.4538	0.3699	0.8815	6.0
H(1D2)	0.5395 (82)	0.3705 (57)	0.9691 (24)	3.4 (16)
H(2D2)	0.7504	0.3550	0.9599	6.0
H(22)	0.932 (10)	0.2397 (73)	0.8154 (29)	5.4 (22)
H(23)	0.782 (11)	0.2090 (76)	0.7398 (33)	7.1 (24)
H(24)	0.581 (10)	0.0328 (74)	0.7389 (30)	5.0 (23)
H(25)	0.514 (10)	−0.0686 (75)	0.8111 (30)	6.9 (24)
H(27)	0.6005	−0.0602	0.9226	6.0
H(28)	0.8420	0.0446	0.9817	6.0
H(29)	0.9585	0.2097	0.9289	6.0

We report briefly here the results of some extended Hückel molecular orbital calculations on (indenyl)Rh$(C_2H_4)_2$ (**2**) and note that our optimized geometry for the ground state is in good agreement with the experimental structure. In particular, the midpoint(olefin)–Rh–midpoint(olefin) angle was 95° (observed 96°), the six-membered ring is tilted 10° from the plane of the three other carbons in the five-membered ring away from the metal (observed 9.0°), and most importantly, the projection of the rhodium atom onto the indenyl plane is slipped 0.18 Å away from an η^5-position toward η^3. Rotation of one ethylene ligand by 90° about the Rh–midpoint(olefin) axis requires 9.3 kcal mol^{-1} which is slightly lower than the 10.3 kcal mol^{-1} that was found experimentally. Concomitantly, the bis(ethylene)rhodium unit slips 0.46 Å from η^5 to essentially an η^3 mode of bonding. The six-membered ring is now bent 20° from the plane of the three carbon atoms in the five-membered ring. There is an electronic reason for the rotational barrier and the attendant distortions. A strong repulsion between a filled polyene π level and a filled metal d orbital is present in any 18-electron polyene–ML_2 complex.[29] This is reduced by a considerable amount by back-bonding to the ethylene π^* orbitals at the ground-state geometry. However, back-bonding is lost when the ethylene is rotated by 90°. The increased repulsion at the transition state can be diminished somewhat by slipping the ML_2 unit to an η^3 geometry. An analogous argument can be advanced for the rotational barrier about the indenyl–Rh axis. We compute an 11.6 kcal mol^{-1}

---

(28) Marder, T. B.; Calabrese, J. C.; Roe, D. C.; Tulip, T. H. *Organometallics*, submitted for publication.

(29) (a) Radonovich, L. J.; Koch, F. J.; Albright, T. A. *Inorg. Chem.* **1980**, *19*, 3373. (b) Byers, L. R.; Dahl, L. F. *Ibid.* **1980**, *19*, 277. (c) Mingos, D. M. P.; Welch, A. J. *J. Chem. Soc., Dalton Trans.* **1980**, 1674. (d) Lichtenberger, D. L.; Belvins, C. H., II; Ortega, R. B. *Organometallics* **1984**, *3*, 1614. (e) Lichtenberger, D. L.; Calabro, D. C.; Kellog, G. E. *Ibid.* **1984**, *3*, 1623.

barrier, but further optimization of the transition state geometry may lower this value. A full account of the bonding and rotational barriers in indenyl–ML_2 complexes is deferred to another paper.

Experimental Section

^{1}H NMR spectra were acquired by using Bruker WH90, WM250, WM400, or AM500 spectrometers; ^{13}C spectra were obtained on a Bruker AM500 spectrometer operating at 125.7 MHz. Mass spectra were obtained by using a VG-7070F mass spectrometer fitted with a VG 2035 data system. Analyses are from Guelph Chemical Laboratory, Guelph, Ontario.

Syntheses of Bis(ethylene)(η^5-indenyl)rhodium(I) (2) and Its 1-Methylindenyl Analogue 3. 2 was synthesized by the method described by Green et al.[8,30] Similarly, treatment of $[(C_2H_4)_2RhCl]_2$ with (1-methylindenyl)lithium yields yellow crystals (from hexane at −78 °C) of **3** (49%): mp 79 °C; ^{1}H NMR (CD_2Cl_2, 293 K) δ 1.85 (s, 3 H, Me), 1.88–1.98 (m, 8 H, C_2H_4), 5.03 (d, 1 H, H^3, J(Rh–H) = 2.7 Hz), 5.99 (t, 1 H, H^2, J(Rh–H) = 2.2 Hz), 7.13–7.28 (m, 4 H, H^{4-7}); ^{13}C NMR (CD_2Cl_2, 293 K) δ 9.8 (Me), 45.7 (d, C_2H_4, J(Rh–C) = 12.3 Hz), 76.7 (d, C^3, J(Rh–C) = 5.1 Hz), 88.8 (C^1), 93.3 (d, C^2, J(Rh–C) = 5.4 Hz), 112.1, 112.9 (C^8, C^9), 117.9, 119.9 (C^4, C^7), 123.6, 123.7 (C^5, C^6); mass spectrum, m/z (relative intensity) 288 (5, P^+), 260 (14, $P - C_2H_4$), 232 (60, $P - 2C_2H_4$). Anal. Calcd for $C_{14}H_{17}Rh$: C, 58.35; H, 5.95. Found: C, 58.65; H, 6.09.

Collection of X-ray Diffraction Data for $(C_9H_7)Rh(C_2H_4)_2$. A dark yellow crystal of $(C_9H_7)Rh(C_2H_4)_2$ was sealed into a 0.2-mm diameter thin-walled glass capillary. The capillary was then mounted (with beeswax) into into an aluminum pin and inserted into a three-directional (XYZ) goniometer on the Syntex P2$_1$ automated four-circle diffractometer at SUNY—Buffalo. All subsequent operations (crystal alignment, determination of unit cell parameters and the crystal's final orientation matrix, data collection) were performed by the previously described techniques of this laboratory.[31] Details appear in Table IV.

Careful inspection of the data set revealed the systemic absences $h0l$ for $h + l = 2n + 1$ and $0k0$ for $k = 2n + 1$ which are consistent with space group $P2_1/n$, a nonstandard setting of the centrosymmetric space group $P2_1/c$ [C_{2h}^5; no. 14].

The data were corrected for the effects of absorption and for Lorentz and polarization factors and were reduced to unscaled $|F_o|$ values. Those reflections with I(net) < 0 were assigned a value of $|F_o| = 0$. A Wilson plot was used to place the data on an approximate absolute scale.

Solution and Refinement of the Structure for $(C_9H_7)Rh(C_2H_4)$. All crystallographic calculations were performed on the SUNY—Buffalo modified version of the Syntex XTL structure solution package. The analytical scattering factors for the neutral atoms were corrected for both the real ($\Delta F'$) and imaginary ($i\Delta f''$) components of anomalous dispersion.[32] The function minimized during least-squares refinement was $\sum w(|F_o| - |F_c|)^2$ where $w^{-1} = [\sigma(|F_o|)]^2 + [0.015|F_o|]^2$.

The structure was solved by using MULTAN, the positions of the two independent rhodiums being determined from an "E map". The remaining non-hydrogen atoms were located from a series of difference-Fourier syntheses. Hydrogen atoms were either located directly from a difference-Fourier map or were placed in calculated positions with d(C–H) = 0.95 Å.[33] Convergence was reached with $R_F = 5.8\%$, $R_{wF} = 4.5\%$, and GOF = 1.32 for 329 parameters refined against 2913 unique data (two data records with errors were omitted—these were the 011 and $56\bar{4}$ reflections). [We note that $R_F = 4.4\%$ and $R_{wF} = 4.3\%$ for those 2464 reflections with $|F_o| > 3\sigma(|F_o|)$, $R_F = 3.6\%$, and $R_{wF} = 3.9\%$ for those 2118 reflections with $|F_o| > 6\sigma(|F_o|)$.]

Final positional parameters are collected in Table V. Anisotropic thermal parameters (Table 5S) and a table of observed and calculated structure factor amplitudes appear as supplementary material.

Extended Hückel Calculations. Extended Hückel molecular orbital calculations were carried out according to the method of Hoffmann.[34] A discussion of the computational details and parameters will be given elsewhere.

Acknowledgment. Financial support from the Natural Sciences and Engineering Council of Canada (M.J.M.), the National Science Foundation (M.R.C.), and the Robert A. Welch, Alfred P. Sloan, and Petroleum Research Foundations (T.A.A.) is gratefully acknowledged. M.M. is the recipient of an NSERC postgraduate scholarship.

Registry No. 2, 63428-46-6; 3, 69074-22-2; $[(C_2H_4)_2RhCl]_2$, 12081-16-2; (1-methylindenyl)lithium, 55563-47-8.

Supplementary Material Available: Tables of anisotropic temperature factors and structure factors (15 pages). Ordering information is given on any current masthead page.

---

(30) The synthesis of $(C_9H_7)Rh(C_2H_4)_2$ also yielded appreciable quantities of an unknown orange product. Its elemental analysis and ^{1}H and ^{13}C NMR spectra matched those obtained for $(C_9H_7)Rh(C_2H_4)_2$. However, mass spectral results under both EI and CI conditions gave peaks at m/e 436 and 333. The possibility exists that it represents some dimeric form of $(C_9H_7)Rh(C_2H_4)_2$. Efforts are continuing to determine the nature of this product.

(31) Churchill, M. R.; Lashewycz, R. A.; Rotella, F. J. *Inorg. Chem.* **1977**, *16*, 265.

(32) *International Tables for X-Ray Crystallography*; Kynoch Press: Birmingham, England, 1974; Vol. 4, pp 99–101, 149–150.

(33) Churchill, M. R. *Inorg. Chem.* **1973**, *12*, 1213.

(34) $R_F = 100\sum||F_o| - |F_c||/\sum|F_o|$, $R_{wF} = 100[\sum w(|F_o| - |F_c|)^2/\sum w|F_o|^2]^{1/2}$, and GOF = $[\sum w(|F_o| - |F_c|)^2/(NO - NV)]^{1/2}$, where NO = number of observations and NV = number of variables.

(35) Hoffmann, R. *J. Chem. Phys.* **1963**, *39*, 1397.